

## Dynamic Analysis Of Two Phase Induction Motor Using Finite Element Method

Edet. G. Ekpo,

Department of Electrical/Electronics Engineering,  
Akwa Ibom State Polytechnic, Ikot Osurua, Ikot Ekpene.

---

### Abstract

The paper presents the dynamic analysis of two phase induction motor with symmetric and orthogonal phase windings. The proposed motor winding arrangement is obtained by making the main and auxiliary windings of a single-phase induction motor equals in all parameters, and connected to a two-phase power sources. The two-phase supply is obtained from the conventional single-phase power supply by using a two-phase inverter drive. Based on geometric dimensions, the model was created using 2D ANSYS Maxwell Finite Element Analysis Software. The transient and steady state analysis of the machine currents, electromagnetic torque and speed on no-load and full-load condition were observed and compared with that of capacitor-start capacitor-run single-phase induction motor. The proposed mode of operation allows the single-phase induction motor with two equal stator windings to gain the advantages of the poly-phase induction motor such as heavy starting torque, improved power factor, less torque harmonics and higher rated power.

---

**Keywords:** Two Phase Induction Motor, Steady state and Transient Response, Flux Levels, FEA

---

### INTRODUCTION

Induction motors are widely used in commercial and industrial sector due to the robustness, simplicity and cost-effectiveness [1]. It is commonly divided into two main categories such as single-phase induction motor and three-phase induction motor. Single-phase induction motors operated from single-phase power supply are widely used in domestic, agricultural and industrial applications, especially where three-phase supply is not available. Most household appliance such as refrigerators, washing machines, fans, air conditioners, food mixers, microwave cookers etc are equipped with single-phase induction motor.

Single-phase induction motors (SPIM) have main and auxiliary windings and due to the asymmetry of stator configuration, the air gap magnetic field would be an ellipse one and can be split into a forward rotating field and a backward rotating field [1]–[2]. The backward magnetic field produces a braking torque in the motor, which results in low efficiency, and low output torque. Such field is a source of increased noise and vibrations due to radial forces affecting the stator boring [3].

Capacitor-run SPIM has a permanent capacitor in series with an auxiliary winding to produce starting torque and to enhance its running performance. Fixed capacitor SPIM systems have many disadvantages since its size required for higher torque at locked rotor is large and near base speed is much smaller.

To overcome this problem, a large start-capacitor is connected and centrifugally switched open before the motor reaches its maximum operating speed such in Capacitor-start Capacitor-run SPIM [4]. The time

shift of voltage in the auxiliary winding is usually due to a start-capacitor connected in series with the auxiliary winding. The run-capacitor only improved the machine efficiency at an elliptic magnetic field in the air-gap [2]. This capacitor switches provide different capacitors value in two distinct speed ranges, to improve the performance of SPIM in the complete range, the capacitance value needs to be continuously varied [5].

Therefore, it is not economic to use single-phase induction motor when the rated power exceeds 0.5 kW [6]. Comparatively, CSCR-SPIM efficiency thus is greater than the permanent connected start-capacitor motor, but less than three-phase induction motor of the same capacity.

Three-phase induction machines are powered by three-phase symmetrical voltage, and the windings are display within the stator and mutually shifted by 120 electrical degrees [7]. These machines operate with circular magnetic fields revolving at a synchronous speed and exhibited heavy starting torque, improved power factor and efficiency, less torque harmonics and higher rated power.

Many researchers have been venture into area of improving efficiency of single-phase induction motor; [8] proposed a novel energy efficient single-phase induction motor, which has three series-connected windings and two capacitors, which make a three-phase induction motor operate from single-phase power supply. [9] Describes a new indirect current control scheme to control the VSI to imitate a dynamic capacitor for low cost open loop control of SPIM. The dynamic capacitance so created extracts

the maximum available torque from the machine. The proposed indirect current control scheme can easily be attached to already existing system without modification in the equipment. The main and auxiliary winding currents are maintained in the phase quadrature by an indirect current control of VSI to realize the maximum torque from the machine.

SPIM can as well be rearranged to have two-phase windings in its stator slots (i.e. a winding layout with two symmetric and orthogonal phase-windings), where both windings exhibiting same characteristics [10], and if powered by two-phase power supply which is spatially space by 90 electrical degree, the machine operate with a circular magnetic field revolving at synchronous speed and exhibit characteristic similar to a three-phase induction motor of the same capacity and vibrations and unfavourable noise are thus suppressed. As the AC power lines are available only in single or three-phase systems, a two-phase voltage system is realized through the use of inverters with different control strategies [11]. This paper presents the dynamic analysis of two-phase induction motor (TPIM) using finite Element Method. This numerical method is more suitable for the electromagnetic field analysis of electric machines; such as complex geometries, magnetic and electric materials, induced currents, coupling of thermal and mechanical effects [12].

**Mathematical Model**

Fig. 2.0 is a four pole two-phase induction motor (TPIM) with two-phase stator windings, portrayed by orthogonal sinusoidal distributed windings with equal windings in the stator slots, which implies that both windings are symmetrical. The axes of the main and auxiliary windings in the case of SPIM are already orthogonal. For simplicity in analysis, the stationary a-b axes may be aligned with the orthogonal axes of the physical winding as shown in Fig 1.

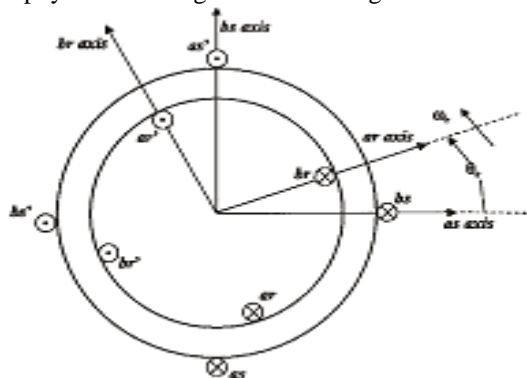


Figure 1: Cross-sectional view of TPIM arranged in space quadrature

The mathematical model describing the operation of electrical machines is a boundary value problem because of the distributed nature of electromagnetic

fields within the machines. It is also an initial value problem because of the time varying field and the source. In addition, the circuit equations should be used to describe the power supply and the connection of windings.

In the model, two types of conductors are considered: solid conductors in which eddy current can be induced, and stranded conductors (windings) without eddy currents. For an electromagnetic problem involving motion, it is advantageous to write the field equations for rotor and stator in their own coordinate systems so as to avoid the rotational speed term appearing explicitly in the formulation and to preserve the symmetry of the final matrix of equations. Thus, the time dependent magnetic diffusion equations are:

$$\nabla \times v \nabla \times A = J_s - \sigma \frac{\partial A}{\partial t} + \sigma \nabla V + V \times H_c$$

where A and V are magnetic vector potential and electric scalar potential, respectively, H<sub>c</sub>, is the coercivity and represents the contribution from permanent magnet, J<sub>s</sub>, is the source current density. For a two dimensional problem, the vectors have only one component in z-direction. In this case, the scalar potential V has a constant value on the cross section of a conductor, and the gradient of the scalar potential can be expressed by the voltage difference, V<sub>b</sub>, across a conductor between the far and near ends. Stranded conductors are normally connected to produce windings. To represent a voltage fed device, circuit equations must be coupled with the field equations. By applying Kirchoff's law, one can write the following circuit equation to relate the terminal voltage U<sub>s</sub>, of a winding to its terminal current I<sub>f</sub>.

$$d_f \frac{N_f^1}{S_f \cdot a} \iint \frac{dA}{dt} \cdot d\Omega + R \cdot i_f + L \cdot \frac{di_f}{dt} + U_C = U_s$$

where N<sub>f</sub> is the total conductor number in this winding, a is the number of parallel branches in the winding, d<sub>f</sub> is the polarity index (+1 or -1) representing forward and return paths; S<sub>f</sub> denotes the total area of the cross section of this coil group. R and L are equivalent resistance and inductance respectively, since they can also include external impedance connected with the winding in addition to the DC resistance and end-turn leakage inductance of the winding itself. U<sub>C</sub>, is the voltage drop across a capacitor. In order to avoid integration due to the inclusion of capacitance, it is necessary to introduce another differential equation to relate capacitor voltage U<sub>C</sub>, to the current i<sub>f</sub>

$$i_f = C \frac{dU_C}{dt} = 0$$

Solid conductors, as used for the rotor bars of an induction motor, are large enough to model skin effects with finite elements. Furthermore, these conductors may be connected at both ends by means of end rings. In order to take end effects into account,

every portion of the ring located between two bars may be considered as external impedance. By taking the squirrel cage as a poly-phase circuit [13], one can obtain the following circuit equations

$$r_e \{i_b\} + l_e \left[ \frac{di_b}{dt} \right] = -[C][C]^T \{V_b\} \quad \text{and}$$

$$\{U_b\} = -\sigma \left[ \frac{dA}{dt} \right] + \frac{\sigma}{l} [V_b]$$

where  $r_e$  and  $l_e$ , are the resistance and the inductance of a portion, between two bars, of the ring respectively,  $[C]$  is the connection bar matrix,  $i$  and  $J$ , are current and current density in the bars respectively.

The equation of motion is

$$J\alpha + \lambda\omega = T_{em} + T_{app}$$

where  $\alpha$  is the angular acceleration,  $\omega$  is the angular velocity,  $J$  is the moment of inertia,  $\lambda$  is the coefficient of friction,  $T_{em}$  is the electromagnetic torque and  $T_{app}$  is the external applied mechanical torque. External applied torque may either be load torque or may be an accelerating driving torque in the same direction as the electromagnetic torque. The sign of both the electromagnetic torque and the

external applied torque is determined by the torque direction, where the anti-clockwise direction is positive and the clockwise direction is negative. At each time step, the electromagnetic torque is computed using the method of virtual work. The rotor angular acceleration, the angular velocity and the displacement is obtain by solving the equation of motion.

This angular displacement is in turn used to move the rotor to a new position. The rotor movement is taken care of by the moving surface method. The basic idea is to create two independent meshes sharing a common moving slip surface, which allows the stationary and moving parts to move freely with respect to each other. Essentially, the moving surface can be imagined to be split into two surfaces. One side is attached to the stationary mesh; the other is attached to the moving mesh. After any specified angular displacement of moving part, the two independent meshes are then coupled together by the finite element shape functions. Thus, part of the mesh is free to move to any specified angle without any remeshing.

Table 1: Electrical and Mechanical Parameter for the 2D Induction Motor design

Parameter	Value
Stator outer dimension	165mm
Stator inner dimension	96mm
Rotor outer dimension	95.6mm
Rotor inner dimension	34mm
Stator number of slots	36 slots
Rotor number of slots	33 bars
Voltage source ; Phase Voltage	230V
Frequency	60Hz
Resistance/Phase A and B (TPIM)	2.36723 $\Omega$
Inductance/phase A and B (TPIM)	0.00320273mH
Resistance/Phase main and Aux.	3.367 $\Omega$ ; 1.367 $\Omega$
Inductance/Phase Main and Aux.	0.0022H; 1.367H
Winding type	Double
Pole pitch	8 slots
Number of turns (TW-IM) Phase A and B	140: 140 turns
Number of turns (SPIM) main and auxiliary	164: 96 turns
Conductor size	0.6mm
Rotor end ring; Inter-bar resistance	2.23717 $\mu\Omega$
Inter-bar inductance	0.0876988 $\mu\text{H}$
Rotor Load; inertia	0.0015Kg-m <sup>2</sup>
Rotor Bars types	Aluminum

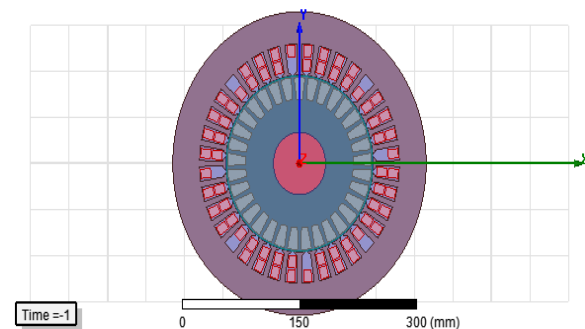


Fig. 2 Model of two-phase motor 2D design of Two-phase induction motor (TPIM)

### MMF Distribution in the Air Gap

In fig 2, the MMF distribution of TPIM is obtained using MATLAB code. The number of turns in stator slots is calculated as shown in fig 3. The main purpose is to observe if the waveforms for the two windings are sinusoidal. This is because the MMF distribution in the air gap is determined by the number of slots and the turns in each slot. From the result of fig 3, they are harmonic component with one fundamental component which is identical with a THD of 0.2173 for both windings.

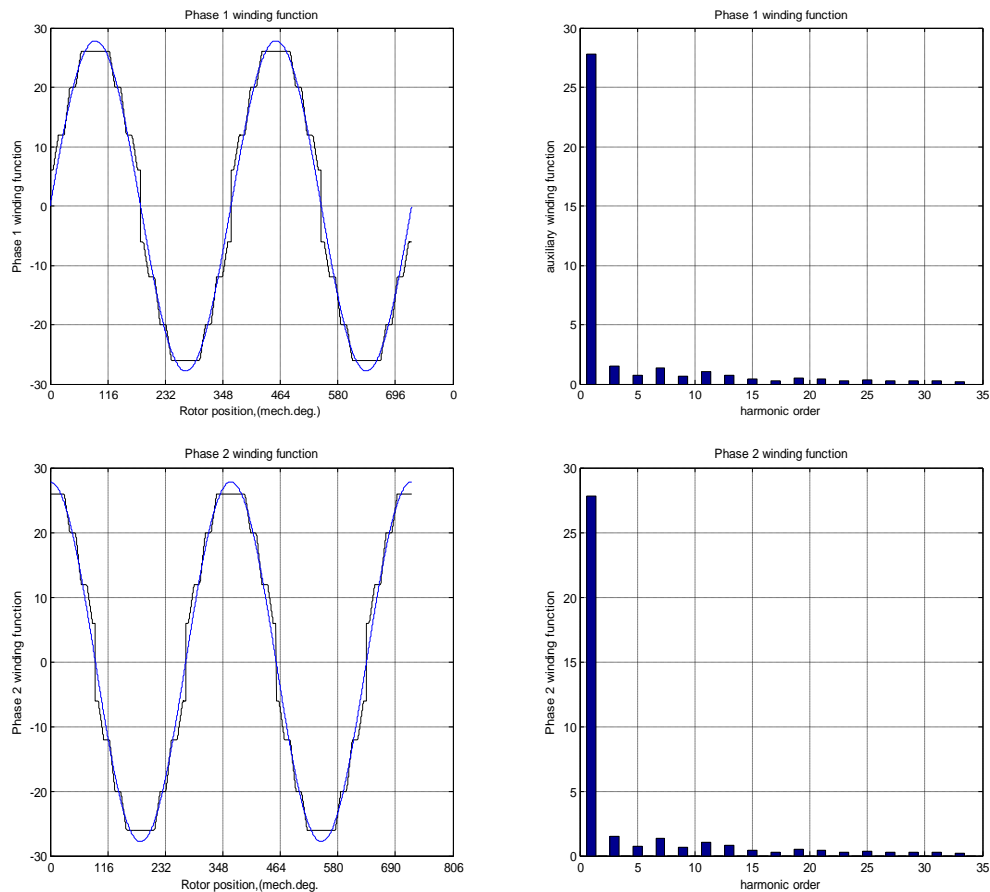


Figure 3: Plot of Winding function diagram for phase 1 and 2 of TPIM and the Harmonic order

**Model of the motor in ANSYS/Maxwell**

The TPIM and SPIM were simulated in the ANSYS/Maxwell program. When directly connected to the

two-phase voltage and line voltage in the case of SPIM the transient was calculated. The motor magnetic field was calculated by the finite elements method in 2D space.

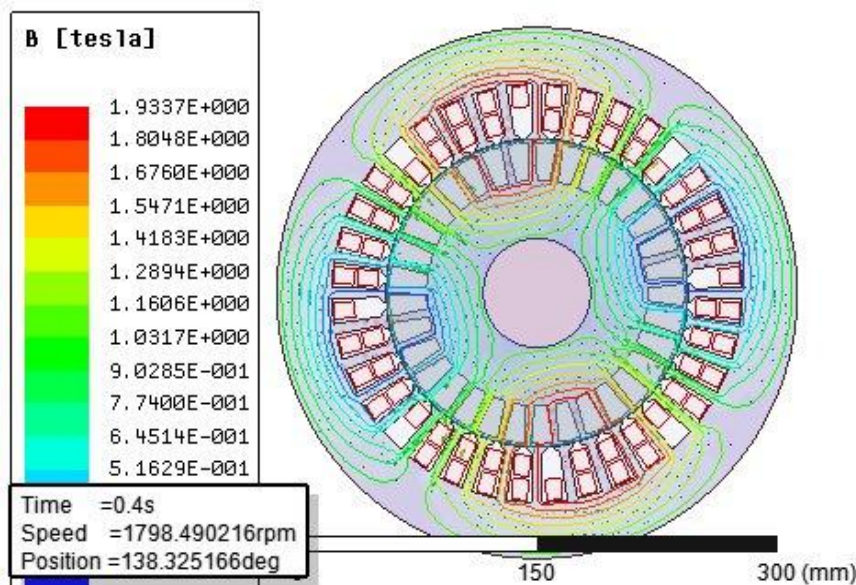


Figure 4: Magnetic field density of motor (Maxwell 2D)

Taken into account at calculating were nonlinear properties of the magnetic circuitry material. In space

illustrated used motor model is shown in Fig. 1. Waveforms of the magnetic field calculated in

Maxwell 2D are shown in Fig. 4 for time  $t=0.4s$ . Distribution of the B- vectors is also calculated for time  $t=0.4s$ , is shown in Fig. 5. The motor is supplied by two-phase symmetrical voltage. Calculated

waveforms of the phase currents, rotor torque and speed are demonstrated in Fig. 6-12 for 2D simulation.

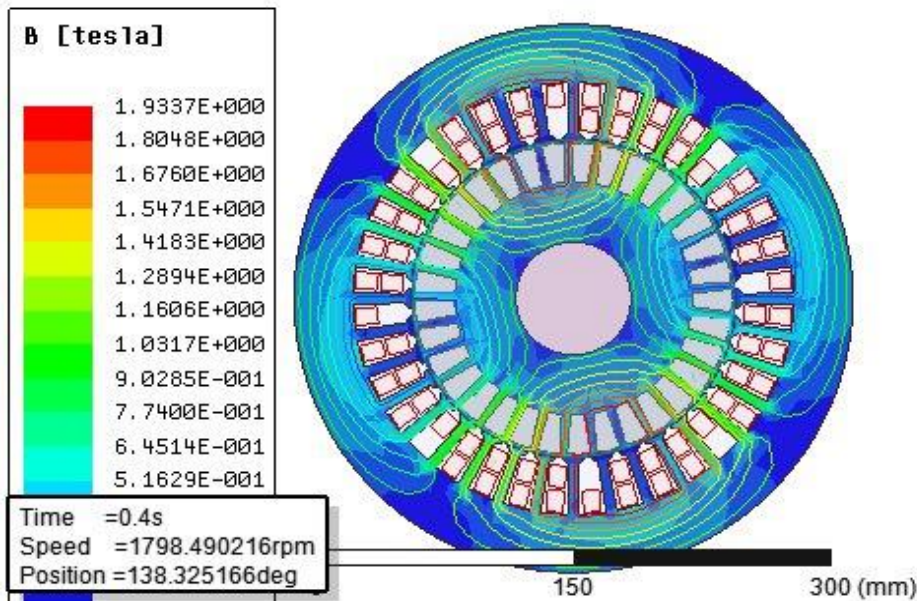


Fig.5 B-vectors calculated by Maxwell 2D for Two-Phase Induction Motor

**Simulation Results for Two-Phase Induction Motor**

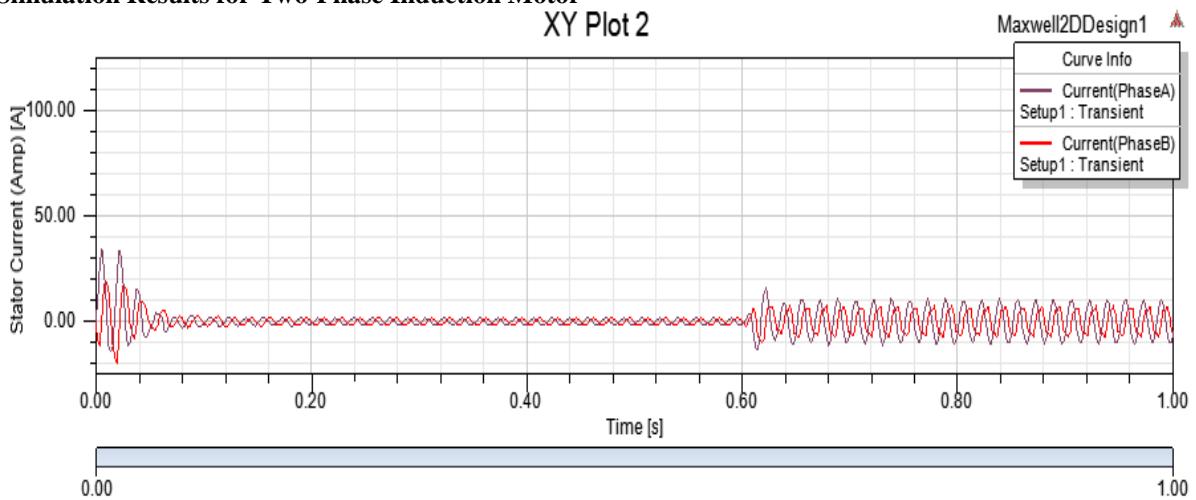


Fig.6 Stator Phase A and B Current showing Transient and steady State respond

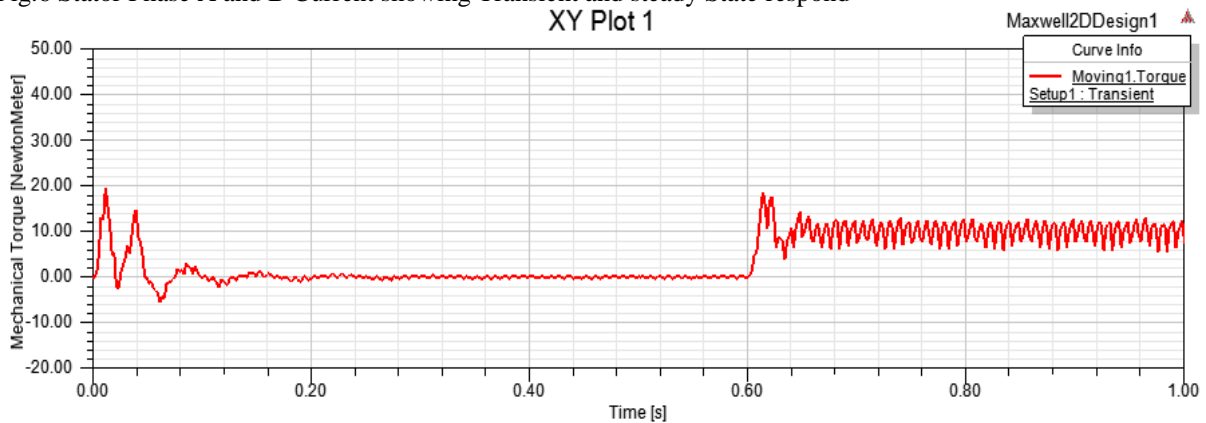


Fig 7 Electromagnetic torque of Two-Phase Induction Motor

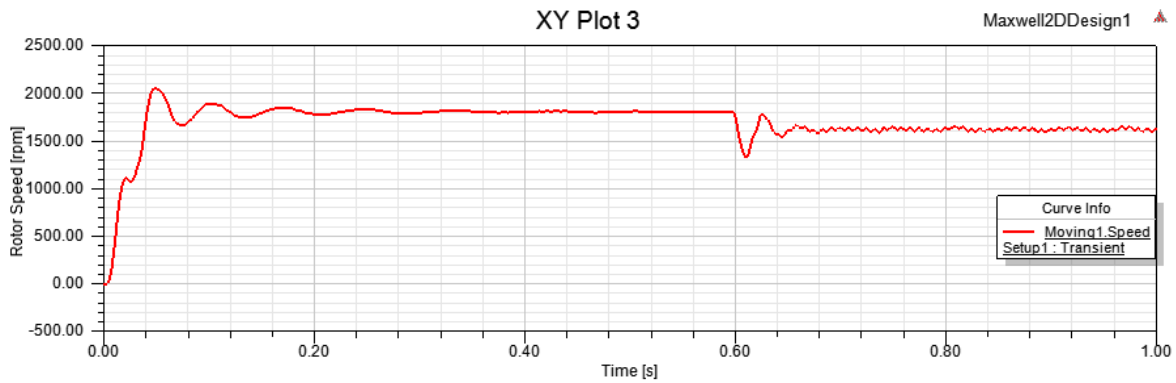


Fig 8 Speed against Time for Two-Phase IM at no load and load conditions

**Simulation Results of Single-Phase Induction Motor:**

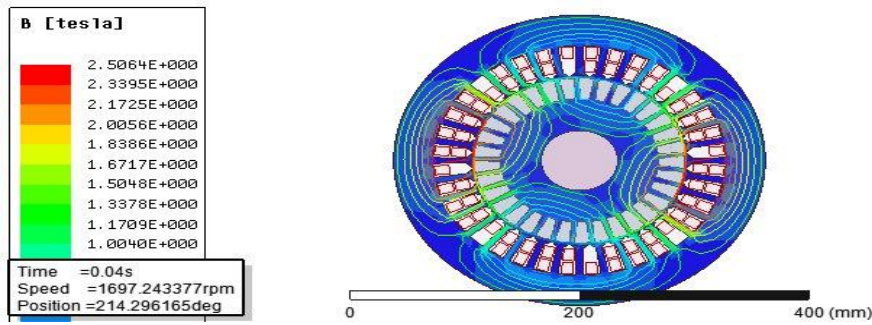


Fig 9 B-vectors calculated by Maxwell 2D for SPIM

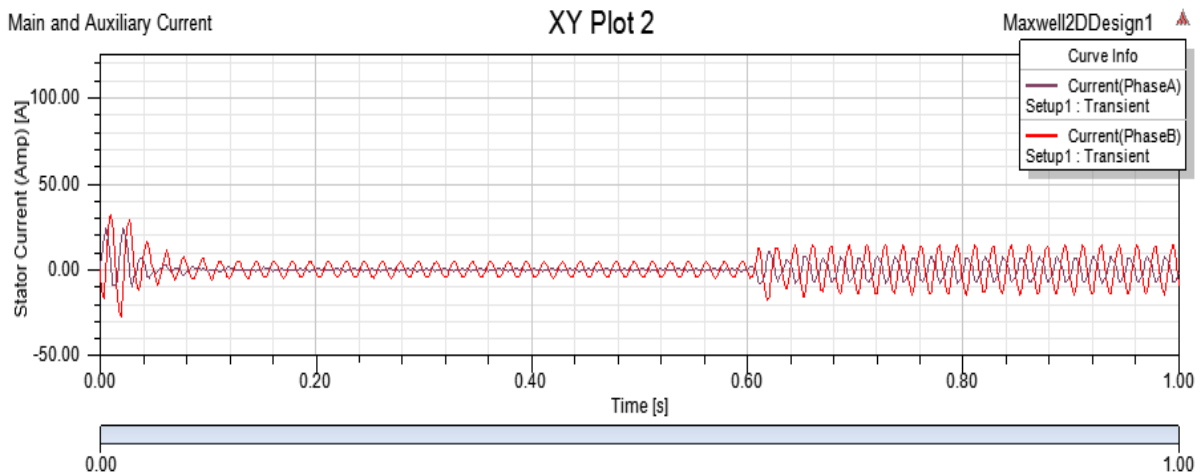


Fig 10 Stator Phase A (Auxiliary) and B (main) Current showing Transient and steady State respond

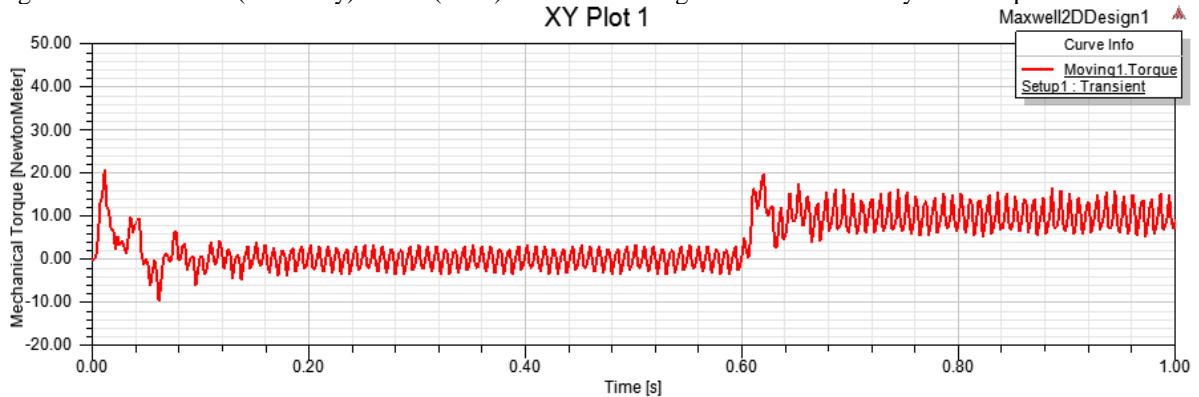


Fig 11 Electromagnetic torque of Single-Phase Induction Motor

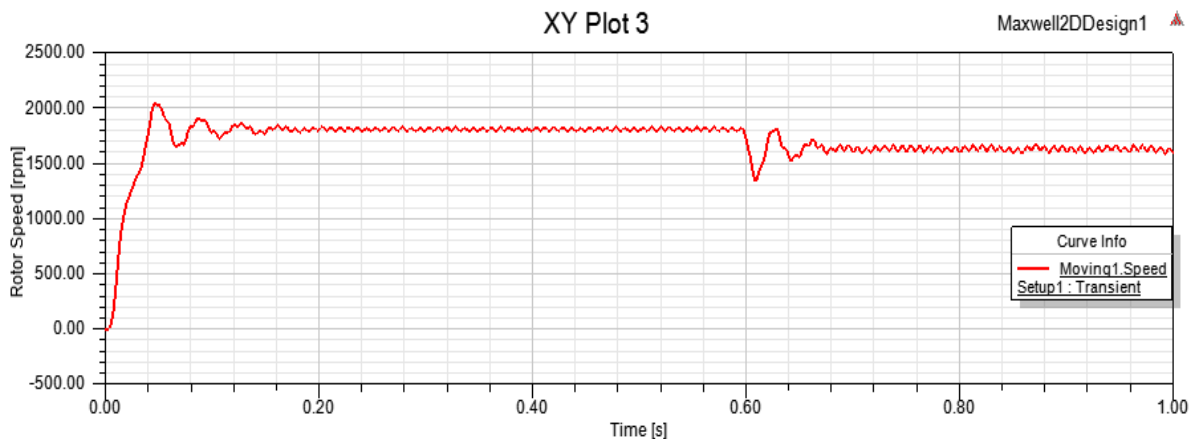


Fig 12 Speed against Time for SPIM at no load and load condition

The figure shows the steady state and transient state of variables such as stator current, rotor speed and electromagnetic torque characteristic at no load and load condition for both two-phase induction motor and single-phase induction motor.

#### No Load Condition

Fig 8 - 12 shows the relationship between the no-load speeds of the rotor with time. The transient and steady state operation is clearly shown in the graph. The two-phase induction motor reached a peak value of about 2044rpm at 0.012 second before it stabilized to 1800rpm at 0.02 second. And also the single-phase induction motor attained its maximum speed of 2032 at 0.04 second and ripple between 1794rpm to 1800rpm at no-load steady state. The machine result in Fig. 6 and 10 shows the waveforms of the stator currents. Fig 6 is the two-phase stator winding current plotted against time while Fig 10 is the main and auxiliary winding stator current plotted against time. Fig. 6 shows a balanced current of 1.7A at steady state as a result of equal number of turns in the TPIM. Fig 10 shows unequal distribution of current between the main (phase B) and auxiliary (phase A) winding as a result of unbalanced winding resulting in higher current of 4.6A at steady state operation. Fig 7 and fig 11 shows that the two motors exhibited nearly equal electromagnetic torque at transient state.

#### Load Condition

In this paper, a load of 10 Nm was introduced at 0.6 second. The behaviour of the two motor was monitored as shown in fig 6 - 12. The stator current rises to 10A in two-phase motor while that single-phase motor recorded 14.7A. Expectedly, the rotor speed in both motor dropped to 1669 rpm and ripples significantly in the SPIM as shown in fig 8 and 12. The electromagnetic torque increases in order to accommodate the load torque. The torque developed in the two-phase motor seen to be higher than the single-phase counterpart. In SPIM, the rotor torque

pulsates at steady state and increases significantly with load than the two-phase motor.

#### CONCLUSIONS

This paper proposed a single-phase induction motor with two equal windings driven with two-phase supply. The proposed configuration granted SPIM the advantages of multiphase machines such as heavy starting torque, high efficiency, higher rated power etc. The currents, torque and speed analysis of the motor performance were reported. The results confirmed that TWO-PHASE SPIM mode of operation provided better performance than CSCR-SPIM. The motor features such as; low IR current; the increased output per current which impact significantly in the running cost in terms of volt-ampere, with reduction on watt per hour cost. It runs smoothly as indicated in the plot of the rotor speed, with little or no ripples, which invariably affect the bearing at long run, noise reduction is of essence, an additional advantage.

#### REFERENCES

- [1] Naser Abdel-Rahim, Adel Shaltout, Operation of Single-phase Induction Motor as Two-phase Motor, *The 28<sup>th</sup> ANNUAL Conference of the IEEE industrial Electronics Society*, vol.2, Nov. 2002,
- [2] Sobhan Sobhani, Hamid Yaghoobi, Mehdi Samakoosh, Optimize Efficiency and Torque in the Single-phase Induction Motor by Adjusting the Design Parameters. *IEEE Environment and Electrical Engineering Conference, EECIC 12<sup>th</sup> international conference on May 2013*.
- [3] V. Hraboveova, L. Kalamen, P. Sekerak and P. Rafajdus, Determination of single-phase motor parameters, *IEEE Power Electronic Electrical Drives Automation and Motor (SPEEDAM) international Symposium*, June 2010.
- [4] Mera R. and Campearu R., Optimal Performances of Capacitor-Run Single-Phase Induction Motor. *IEEE Transaction*, 2012, 718-723.

- [5] H. Huang, E. F. Fuchs, J. C. White, Optimal Placement of the Run Capacitor in Single-Phase Induction Motor Designs, *IEEE Transaction on Energy Conversion*, Vol. 3, No. 3, September 1988.
- [6] E. F. Fushs, A. J. Vandenput, J. Holl, J. C. White, Design Analysis of Capacitor-Start Capacitor-run Single-phase Induction Motors, *IEEE Transaction on Energy Conversation*, Vol.5.No.2, June 1990.
- [7] Ping Zhou, Scott Stanton, Zoltan J. Cendes, Dynamic Modelling of three-Phase and Single-Phase Induction Motors, *Electrical Machines and Drives 1999. International conference IEMD'99*. May 1999. Seattle, WA.
- [8] Li Xinhua, Xiong Hao, Zhou Keding, Starting Process Simulation of Nd-Fe-B single-phase Permanent-Magnet Synchronuos Motor Fed by PWM Inverter, *IEEE Electrical Machines and Systems, 2001. ICEMS 2001 Proceedings of the Fifth International Conference on* (Volume: 2) August 2001.
- [9] Vishal Verma, Peeyush Pant, and Bhim Singh, Simulation of a Single-phase Induction Motor with Dynamic Capacitor for Maximum Torque Operation, *IEEE Power India Conference 2008, Power System Technology conference*, Oct. 2008.
- [10] E. Sorrentino, S. Fernandez, Comparison of six steady-state models for single-phase induction motors, *Published in IET Electric Power Applications*, 1<sup>st</sup> January 2011.
- [11] C van der Merwe, F S van der Merwe, A Study of Methods to Measure the Parameters of Single-phase Induction Motors, *IEEE Transaction on Energy Conversion*, Vol. 10. No. 2, June 1995.
- [12] Salon, S. J. and *Finite Element Analysis of Electrical Machines*; Kluwer Academic Publishers, 1995.
- [13] E. Vassent, G. Meunier and A. Foggia, "Simulation of induction machines using complex magnetodynamic finite element method coupled with the circuit equations", *IEEE, Trans. on Mugnetics*, vol. 27, no. 6, September 1991,pp. 4246-4249.